CHARACTERIZATION OF WET-WOUND INSULATED 2G-HTS TAPE IN A DEWAR*

J. C. Jan†, C. C. Tsai, F. Y. Lin, C. K. Yang and T. Y. Chung
National Synchrotron Radiation Research Center, Hsinchu, Taiwan.

Abstract

The second-generation high-temperature superconductor is under consideration for accelerator applications because its operating temperature, which is higher than 4.2 K, eliminates the need for liquid helium. However, the relatively low engineering critical current, inter-layer insulation challenges, welding reliability and quench protection remain key technical issues. In this work, an insulated high-temperature superconducting tape was wet-wound using a low-temperature adhesive. The winding method, charging behavior, as well as quench protection were experimentally investigated. A simple liquid-helium-free test dewar is also presented.

INTRODUCTION

Second-generation high-temperature superconducting tape (2G-HTS tape) is a promising option for winding accelerator magnets, offering high current density and excellent performance under strong magnetic fields. In addition, HTS materials can operate at higher temperatures, thereby reducing reliance on liquid helium. However, compared with low-temperature superconductors such as NbTi wire, 2G-HTS tape presents greater challenges in winding and electrical characteristics. These include constraints on minimum bending radius, the need to avoid twisting, and difficulties in quench detection. No-insulated (NI), metal-insulated (MI), and insulated (INS) windings have been studied to understand HTS behavior after winding. NI winding suffers from charging delays and shielding current effects; however, its excellent thermal stability enables self-protection during a quench [1, 2]. MI winding has disadvantages including low packing factor, charging delay, contact resistance instability, and complex winding, but its metallic insulation provides a more efficient heat dissipation path during a quench compared to INS winding [2]. INS winding has disadvantages such as a low packing factor, slow quench propagation, thermal mismatch, and insulation delamination. However, it also offers advantages, including predictable electrical paths, no charging delay, and simple current control [1-3]. The final goal of this project is to generate a 3.5 T magnetic field using 12 mm 2G-HTS tape operating at 20 K in a cryogen-free dewar [4]. Considering the relatively low magnetic field requirement and operating current, the insulated (INS) winding method was selected to fabricate a prototype, referred to as HTS-P1-5t. In this study, insulated 2G-HTS tape was wound and fixed using cryogenic epoxy, and then installed in a cryogen-free dewar to evaluate its thermal and charging characteristics.

*Work supported by NSTC
† janjc@nsrrc.org.tw

2G-HTS TAPE WINDING

The HTS-P1-5t was wound using insulated SCS12050-AP-i HTS tape supplied by SuperPower Inc. (Furukawa), with the joints formed by PbSn soldering. The HTS tape is insulated with a 0.025 mm thick layer consisting of polyimide film and silicone adhesive, applied with a 30% overlap. The final average width and thickness of the insulated 2G-HTS tape are 12.04 mm and 0.169 mm, respectively.

Figure 1(a) shows the HTS-P1-5t and the return yoke, with a magnified view of the joint (red box) presented in Fig. 1 (b). The pole and return yoke are fabricated from DT4E pure iron, and a 1 mm thick copper spacer (Cu-spacer) is inserted between the pole and the 2G-HTS tape to prevent the peak magnetic field from concentrating on the tape surface. The Cu-spacer must provide good contact with the pole while maintaining effective heat conduction. Therefore, ten turns of 0.1 mm thick copper sheets are wet-wound directly onto the pole, as shown in Fig. 1(b). A 0.4 mm groove is subsequently machined to solider the 2G-HTS extended leads. After curing of the Cu-spacer, the 2G-HTS tape was wet-wound onto the Cu-spacer. The 2G-HTS tape layers were bonded together using a cryogenic epoxy prepared from GY285 and HY5922. The tension applied during 2G-HTS winding is approximately 2 kgf. In addition, each 2G-HTS extended lead is overlapped with three 2G-HTS tapes to improve mechanical robustness and reliability, as shown in Fig. 1(a). Figure 1(c) shows the HTS-P1-5t installed in a copper cooling housing. The HTS-P1-5t is enclosed by copper on three sides, while one side is intentionally left open to simulate the electron-beam pass-through region, which experiences relatively poor cooling conditions. Cryogenic grease or Indium sheets is applied to all contact surfaces to enhance thermal transfer efficiency. The composition materials of the HTS-P1-5t include DT4E, copper, polyimide film, Hastelloy and cryogenic epoxy. Figure 2 illustrates the material contact arrangement and corresponding thickness within the HTS-P1-5t winding. Table 1 lists the integrated thermal contraction ($\Delta L/L$) of these materials [5-8]. The thermal contraction of the Hastelloy was approximated using the cryogenic contraction data of Inconel 718. The polyimide and cryogenic epoxy are relative soft compared to DT4E or copper. Therefore, these thin soft layers can maintain good thermal contact and buffering small deformations between the metal layers.

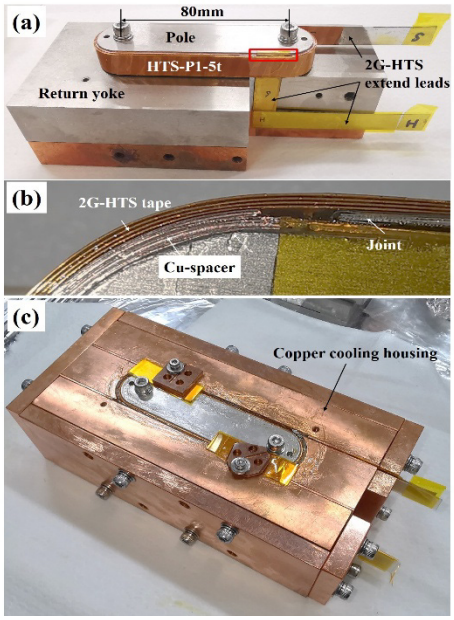

Figure 1: Photographs of (a) HTS-P1-5t prototype, (b) a magnified view of the joint, and (c) the cooling housing.

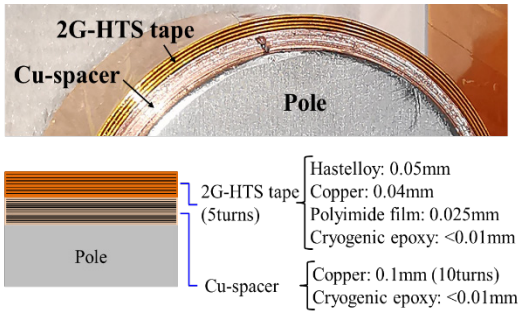

Figure 2: Material contact arrangement and thickness in the HTS-P1-5t winding.

Table 1: Integrated Thermal Contraction of Materials

$\Delta L/L$ ($x10^{-3}$)	300-200 (K)	300-100 (K)	300-20 (K)
DT4E	-1.2	-1.8	-2.1
Copper (RRR50)	-1.5	-3.0	-3.2
Polyimide film	-4.3	-8.5	-11.4
Hastelloy (Inc 718)	-1.2	-2.1	-2.4
Cryogenic epoxy	-5.5	-9.5	-11.5

CRYOGEN-FREE DEWAR SETUP

A liquid-helium-free dewar, denoted as LHFD, was designed for the cool-down and charging of HTS-P1-5t. The structure of the LHFD is illustrated in Fig. 3(a), and a photograph is presented in Fig. 3(b). Two Sumitomo cryocoolers, the RDK-415D and CH-110, were employed to cool the HTS-P1-5t and the 1G-HTS leads, respectively.

The power feedthroughs have a current capacity of 600 A at room temperature, while the 1G-HTS leads have a maximum current capacity of 900 A at 77 K. The 1G-HTS leads prevent joule heating and conductive heat loads from being transferred to the HTS-P1-5t. A total of 14 Cernox temperature sensors were installed in the test dewar, and their locations are indicated in Fig. 3(a). The voltages across the 1G-HTS leads and HTS-P1-5t were monitored at positions e-b and b-c, respectively. An AREPOC HHP-MP Hall sensor was mounted on the pole to measure the magnetic field and verify that the excitation current was properly flowing through the HTS-P1-5t. The green dashed lines represent copper strips used to enhance the cooling performance of the HTS-P1-5t and the 2G-HTS extend leads. In addition, a copper radiation shield was installed to reduce heat radiation from the dewar wall.

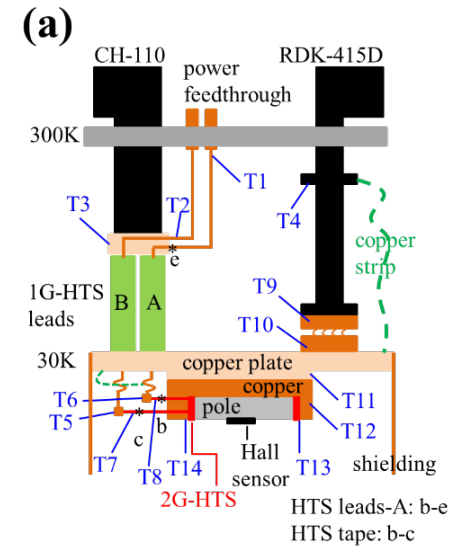

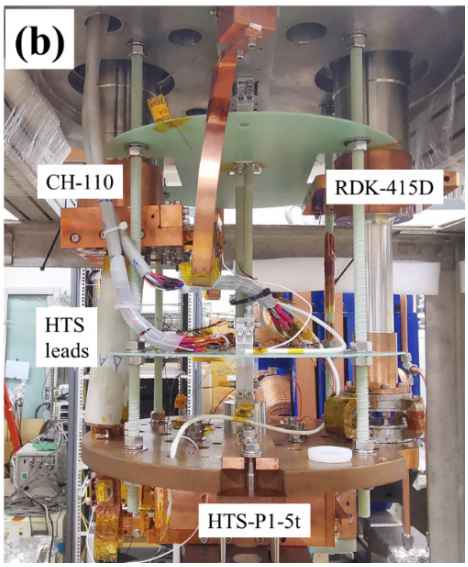

Figure 3: (a) Schematic of the thermal sensor and voltage signal measurement setup, and (b) photograph of the LHFD.

COOL DOWN AND CHARGE

Figures 4(a) and (b) present the total resistance and temperature profiles during the cool-down process. The HTS-P1-5t was cooled down to 50 K within 23 hrs. The steady-state temperatures of T4 (first-stage), T9 (second-stage), T10 (copper plate), T13 (HTS-P1-5t tape), and T14 (HTS-P1-5t tape) were 34 K, 37 K, 39 K, 50 K, and 56 K, respectively (not show in the figure). Therefore, the heat transfer from the copper plate to the first-stage of the RDK-415D cryo-cooler was estimated to be 1.88 W, which corresponds to the static heat load of the LHFD. A superconducting transition of HTS-P1-5t (b-c) was observed in Fig. 4(a) within the temperature range of 80–95 K, as indicated by T13 and T14. The superconducting transition was identified using a two-wire resistance measurement. In addition, the resistance across b-c of the HTS-P1-5t was accurately measured using the four-wire resistance measurement method, yielding values of 0.046 Ω at 300 K and 400 nΩ at 53 K. This measurement includes the contact resistance of one bolted joint. Figure 4(b) shows the copper connectors (T5 and T6) and 2G-HTS extended leads (T7 and T8) were cooled to approximately 63 K and 62 K, respectively. However, heat dissipation in these components remained insufficient because of their small cross-sectional areas.

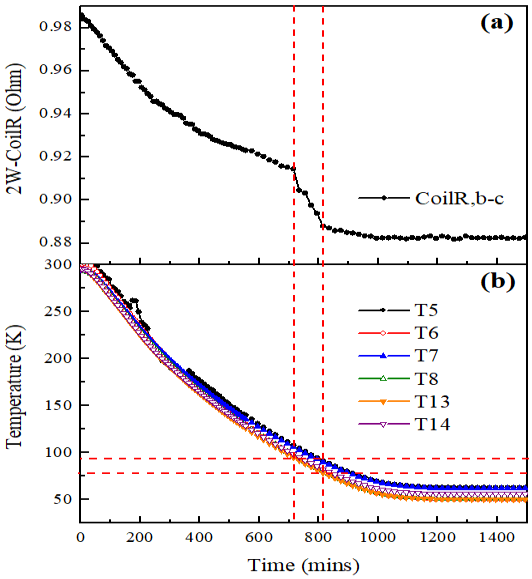

Figure 4: (a) Resistance between b-c measured by the two-wire method and, (b) temperature distribution during cool-down.

Figures 5(a), (b) and (c) present the charging characteristics of the overall circuit, the HTS-P1-5t circuit, the 1G-HTS lead circuit, and the corresponding Hall sensor signal after two thermal cycles. Figure 5(a) shows the current-voltage characteristics of the overall system during three charging processes, with the signals measured at the power supply. Figure 5(b) presents the voltages measured across b-c and b-e, corresponding to the HTS-P1-5t tape and the 1G-HTS lead, respectively. The charging characteristics of these HTS components were similar, indicating that both the HTS-P1-5t and 1G-HTS lead operated normally during the three charging processes. Figure 5(c) shows that the Hall sensor signal is proportional to the excitation current, confirming that the excitation current correctly passed through the HTS-P1-5t tape during the three charging processes. This indicates that the HTS-P1-5t is operating normally. Based on these results, the abnormal system voltage observed in Fig. 5(a) was not associated with the HTS-P1-5t tape and is instead attributed to insufficient heat dissipation in other copper connectors. This issue will be improved in future designs.

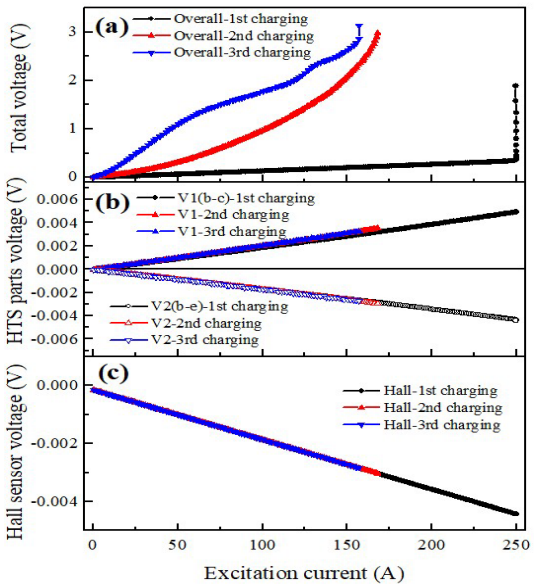

Figure 5: Voltage distribution of (a) the overall circuit, (b) the HTS-P1-5t and 1G-HTS lead, and (c) the corresponding Hall sensor signal during charging.

SUMMARY

In this study, a wet-wound insulated HTS-P1-5t prototype was wound and characterized in a cryogen-free dewar. The prototype reached a stable temperature of 50 K within 23 hrs. A superconducting transition was clearly observed in the temperature range of 80-95 K. In addition, the four-wire resistance measurement of HTS-P1-5t at 53 K yielded a low resistance of 400 nΩ, including the contact resistance of one bolted joint. Furthermore, charging tests verified by Hall sensor signals demonstrated that the excitation current was applied to the HTS tape without degradation after two thermal cycles and three charging cycles. Although the HTS components operated normally, voltage abnormalities were identified in the external copper joints, and insufficient heat dissipation was observed in certain connectors. These findings provide important guidance for the next design iteration.

REFERENCES

[1] B. G. Koshy, M. Ainslie, Y. Sun, B. P. P. Mallett, and Z. Jiang, "Numerical study of dynamic resistance and total loss in insulated and non-insulated HTS REBCO double-pancake coils at 77 K", *Superconductivity*, vol. 16, no. 100216, 2025. doi:10.1016/j.supcon.2025.100216

[2] H. Song, D. Hazelton, D. Fukushima, and P. Brownsey, "Engineering design and novel winding approaches in developing high quality HTS REBCO coils", in *IEEE Trans. Appl. Supercond.*, vol. 27, no. 4, pp. 4601305, June 2017. doi:10.1109/TASC.2017.2652540

[3] G. Messina, M. Yazdani-Asrami, F. Marignetti, and A. della Corte, "Characterization of HTS coils for superconducting rotating electric machine applications: challenges, material selection, winding process, and testing", in *IEEE Trans. Appl. Supercond.*, vol. 31, no. 2, no. 9285175, Mar 2021. doi:10.1109/TASC.2020.3042829

[4] J. C. Jan, C. C. Tsai, P. K. Wang, and F. Y. Lin, "Magnetic circuit design and consideration for HTSW using 12 mm HTS tape", in *Proc. IPAC'25,* Taipei, Taiwan, Jun. 2025, pp.1822-1825. doi:10.18429/JACoW-IPAC2025-WEPB038

[5] S. W. Van Sciver, "Low-Temperature Materials Properties", in *Helium Cryogenics*, 2nd Ed. New York, NY, USA: Springer, 2012, pp.28-29.

[6] P. Duthil, "Material Properties at Low Temperature," CERN Yellow Report CERN-2014-005, pp. 77–95, 2014. doi:10.5170/CERN-2014-005.77

[7] Johnson, V. J. (Ed.) Part II: Properties of Solids. WADD Technical Report 60-56, 1960.

[8] S. Kalia and S.-Y. Fu, Eds., *Polymers at Cryogenic Temperatures*, Springer-Verlag Berlin Heidelberg, 2013. doi:10.1007/978-3-642-35335-2_2